Available online at www.sciencedirect.com
SCIENCE DIRECT®
Ecological Modelling 186 (2005) 43–54
ECOLOGICAL MODELLING
www.elsevier.com/locate/ecolmodel

Modelling the components of the vertical attenuation of ultraviolet radiation in a wetland lake ecosystem

Luca Bracchini [a,*], Andrés Cózar [a,b], Arduino Massimo Dattilo [a], Maria Pia Picchi [a], Carmen Arena [c], Stefania Mazzuoli [a], Steven A. Loiselle [a]

[a] *Department of Chemical and Biosystem Sciences, Laboratory of Environmental Spectroscopy, University of Siena and C.S.G.I, Via Aldo Moro 2, 53100 Siena, Italy*
[b] *Area de Ecología, Facultad de Ciencias del Mar, University of Cadiz, 11150 Cádiz, Spain*
[c] *Department of Vegetal Biology, University of Napoli Federico II, Via Foria 223, 80139 Napoli, Italy*

Available online 8 April 2005

Abstract

The extinction of solar UV (290–400 nm) radiation in aquatic ecosystems is a complex phenomena. In this paper, we examine and model the attenuation of UV radiation in a shallow lake ecosystem. In particular we focus our analysis on the specific role of the fractions of dissolved and particulate matter in the water column in the attenuation of radiation. This analysis is aimed by representing the spatial distribution of each fraction making it possible to evidence the spatial variation in habitat quality. In situ and laboratory measurement are used to elaborate a UV attenuation model. The attenuation model distinguishes between the contribution of particulate and dissolved matter in the attenuation of the solar UV flux. In the studied wetland lake (*Laguna Iberá*, sub-tropical latitude, Argentina) the importance of dissolved matter is dominated in the UVB solar spectrum (290–320 nm) but the effects of the particulate fraction are not negligible, in particular in UVA (320–400 nm). The spatial representation of model results demonstrate the non homogeneous nature between attenuation of the two fractions. Local and global environmental change can have important impacts on dissolved and particulate matter concentrations, which cam have ecological consequences in relation to the high flux of incoming UV radiation. The model developed to examine the relative attenuation of the dissolved and particulate fractions and is a useful instrument to identify the role that these fractions have on the optical characteristics of aquatic ecosystems.

Keywords: UV attenuation model; Aquatic ecosystem; Dissolved and particulate matter

1. Introduction

The quantity and quality of electromagnetic radiation within an aquatic ecosystem has important effects on the biological and physical chemical conditions that permit the system to evolve. The interaction of the solar UV (290–400 nm) and visible (400–700 nm) wavelengths with the ecosystem has elicited a number of important research efforts (Hader et al., 1998; Kirk, 1977; Bothwell et al., 1994). The fate of the electromagnetic radiation within the medium in these solar spectral ranges depends on the components

* Corresponding author. Tel.: +39 0577 234369; fax: +39 0577 234177.
E-mail address: bracchini@unisi.it (L. Bracchini).

0304-3800/$ – see front matter © 2005 Elsevier B.V. All rights reserved.
doi:10.1016/j.ecolmodel.2005.03.001

of the water medium, as well as the changes in the radiation environment above the water line and the condition of the water surface. To determine the quantity of available radiation within the water body, an attenuation coefficient can be calculated based on the measurement of the energy flux at different depths. The attenuation coefficient depends on the chemical and physical characteristics of that column of water in which it is determined. Besides the water itself, the role of the dissolved and particulate matter plays the most important role in attenuation (Kirk et al., 1994; Morris et al., 1995; Nieke et al., 1997; Bracchini et al., 2004a).

Interest in the effect of UV radiation and its impact on the aquatic environment has increased in recent years. This is mostly due to the reduction of the stratospheric ozone layer but also due to the modification of the aquatic environment due to local and regional pollution (Yan et al., 1996; Schindler et al., 1996; Pienitz and Vincent, 2000; Bracchini et al., 2004b). Impacts on the biotic (Dattilo et al., 2005a; Hakkinen et al., 2001; Smith and Baker, 1978) and abiotic community (Amyot et al., 1997; Dattilo et al., 2005b) have been measured to be potentially relevant. The impact of specific components of the aquatic ecosystem on the attenuation of UV radiation has been noted (Kirk, 1994). The present work is dedicated to modelling the role of the major water components in the attenuation of UV radiation within a shallow lake (*Laguna Iberá*). The study site is located in a Ramsar wetland of international importance in South America (*Esteros del Iberá*).

2. Study site

The present study was conducted in the *Esteros del Iberá* wetland, in northeast Argentina and in particular in *Laguna Iberá*, which is located at 28°S and 57°W. The surface is 54 km^2. It is permanent lake with an average depth of 3.0 m and a maximum of 4.5 m. The lake is divided in two basins (northern and southern basin, Fig. 10) has two small inlets which drain extensive wetland areas, and strongly influence the water quality in the lake. The lake is surrounded by floating vegetation mats, that extend up to 1000 m in width and 2 m in depth and consist of decaying vegetation which is in contact with water below and on each side.

3. Materials and methods

The campaign was performed in October 2001 during austral mid-spring. Seventy seven stations were selected to cover the entire surface of *Laguna Iberá*. In each site, a vertical profile of the UV irradiance was measured using a PUV541 spectroradiometer SN 19235 (Biospherical Instruments, San Diego, CA). The instrument was calibrated during July 2001, by comparing the measured irradiances of the instrument with a second spectroradiometer with 1 nm of spectral resolution (SUV spectroradiometer, Biospherical Instruments, San Diego, CA). The PUV541 was connected to a portable battery and a portable computer with a specific programme to collect the flux data. The instrument was lowered into the water column and measurements of UV radiation, water temperature and water depth were acquired simultaneously every 0.3 s. The time required for each profile was 4 min (downward and upward). The spectral irradiance was measured at 305 nm (bandpass 7 nm), 313 nm (bandpass 10 nm), 320 nm (bandpass 11 nm) and 340 nm (bandpass 10 nm). The noise of the sensors is of the order of 0.001 $\mu W/(cm^2\ nm)$. Measurements were made between 10:30 and 15:30 in days with limited cloudiness and low wind. The geographical location of each sampling point was recorded using a GPS (Garmin GPS III). The measurements were initiated below the water line (0.02 m) and the measurements were recorded while the instrument was lowered to the lake bottom as well as during the raising of the instrument just below the water surface. On average, 60 measurements were use in each station. The resulting radiation profile was corrected by removing the instrument dark current and temperature effect and plotted against water depth. All profiles in which the R^2 of the exponential fitting was less than 0.40 were discarded.

Simultaneously to the radiation profile measurements, water sample were collected at a depth of 0.30 m. The water samples were filtered using a GV Millipore 0.22 μm filter. The samples are stored in the dark at 4 °C and analysed using a UV–vis spectrophotometer (Ultraspec 2000, Pharmacia Biotech). The spectral extinctions values (a_λ, dimensionless) was recorded for each samples at 305, 313, 320, and 340 nm.

4. Results

The optical properties of a water medium depend largely upon the characteristics of the dissolved and particulate matter of the medium, which influence the absorption and scattering of the incoming radiation. The sum of the absorption and the scattering is considered the attenuation (or extinction, m^{-1}). When considering this loss of energy along the water column, the radiant flux will diminish in an exponential curve, according to the Lambert–Beer law (Eq. (1)).

$$I_\lambda = I_{0,\lambda} \exp(-K_{d,\lambda}(z - z_0)) \quad (1)$$

where $I_{0,\lambda}$ and I_λ [μWatt cm^{-2} nm^{-1}] are the spectral irradiance at $z_0 = 0.02$ m, and at depth z [m]. $K_{d,\lambda}$ [m^{-1}] is the total attenuation coefficient for downward radiation. The $K_{d,\lambda}$ coefficient considers both the absorptive and scattering properties of the medium in the direct measure of the attenuation of the available radiation with depth (Figs. 1–4).

To examine the role of dissolved matter in the total vertical attenuation, the extinction spectrum of the filtered samples was determined using a spectrophotometer. The absorption of the dissolved matter can be explained with the electronic transition of the type $\pi \rightarrow \pi^*$ which occurs in the region between about 270 and 280 nm for benzoic acids, aniline derivates, polyenes and polycyclic aromatic hydrocarbons with two or more rings. For spectrophotometric analysis of these compounds, wavelengths from 272 to 465 nm have been used (Kirk, 1994). The wavelength 272 nm can be used to obtain an estimation of all the dissolved organic matter present in the water sample, comprising not only humic and fulvic acids, but also decomposition products of semi-stable organic materials in solution. Theoretically (Kirk, 1994), the spectral extinction can be related to the extinction coefficient of the dissolved fraction (diameter < 0.22 μm) by converting the a_λ measurement to m^{-1} (Eq. (2)).

$$\frac{2.3 \times a_\lambda}{10^{-2}} = A_\lambda \quad (2)$$

where the factor 2.3 converts the decimal logarithm of the spectrophotometer extinction measurement to the natural logarithm of the in situ attenuation measurement. The factor 10^{-2} converts the cuvette width of 1 cm to meters. Therefore A_λ (m^{-1}) measures the extinction of the dissolved matter in the collected samples according $K_{d,\lambda}$ unit.

As the vertical attenuation coefficient sums the contribution of the extinction due to both dissolved matter and particulate matter in the water column, changes in the extinction due to the dissolved fraction should relate to the total vertical attenuation in the following

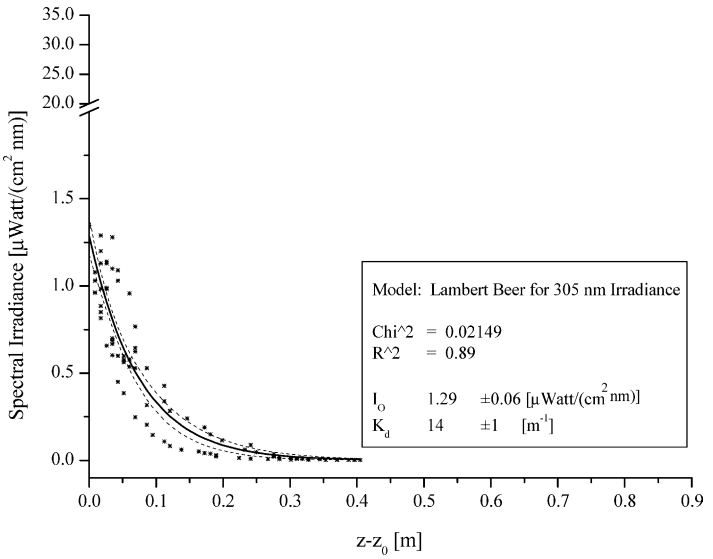

Fig. 1. Spectral irradiance at 305 nm plotted against corrected depth ($z - z_0$) according to Eq. (1) (continuous line = model of Eq. (1); scattered line = 95% confidence band). All errors are calculated from 95% confidence band.

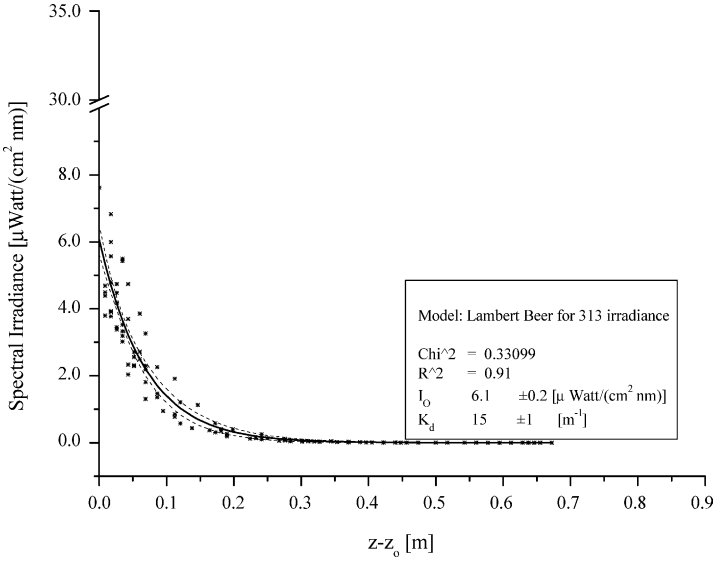

Fig. 2. Spectral irradiance at 313 nm plotted against corrected depth ($z - z_0$) according to Eq. (1) (continuous line = model of Eq. (1); scattered line = 95% confidence band). All errors are calculated from 95% confidence band.

manner:

$$K_{d,\lambda} = A_\lambda + K_{p,\lambda} \tag{3}$$

where $K_{p,\lambda}$ (m^{-1}) is the extinction coefficient of the particulate fraction of the water column. The above model for the vertical attenuation may be further elaborated to directly include the measured extinction from the spectrophotometer.

$$K_{d,\lambda} = \frac{2.3 \times a_\lambda}{10^{-2}} + K_{p,\lambda} \tag{4}$$

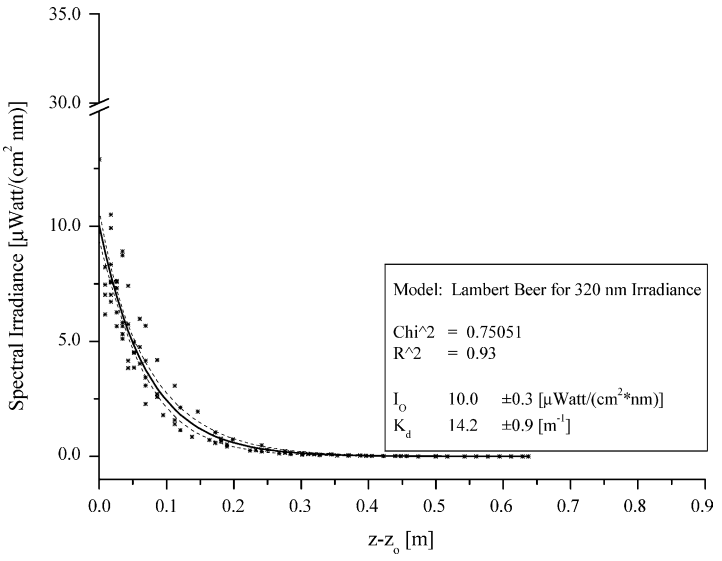

Fig. 3. Spectral irradiance at 320 nm plotted against corrected depth ($z - z_0$) according to Eq. (1) (continuous line = model of Eq. (1); scattered line = 95% confidence band). All errors are calculated from 95% confidence band.

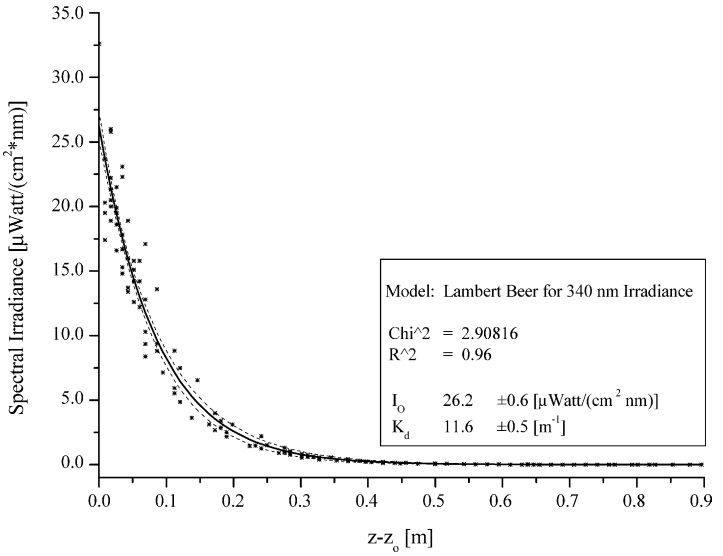

Fig. 4. Spectral irradiance at 340 nm plotted against corrected depth ($z - z_0$) according to Eq. (1) (continuous line = model of Eq. (1); scattered line = 95% confidence band). All errors are calculated from 95% confidence band.

If the vertical attenuation $K_{d,\lambda}$ is dominated by the concentration of the dissolved matter, Eq. (4) will be nearly linear. To examine this approach, $K_{d,\lambda}$ and the a_λ of the 77 sampled stations were plotted, for each wavelength (Figs. 5–8) measured by the spectroradiometer.

The intercept to the least square method (b values) could be considered the average contribution to UV radiation attenuation of the particulate matter for the whole lake.

The angular coefficients estimated by the measured attenuation and the absorbance in four wave-

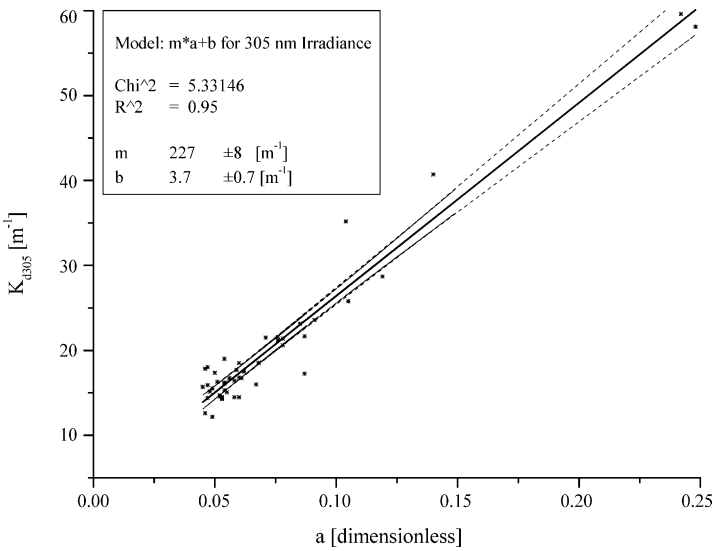

Fig. 5. Linear regression between $K_{d,305}$ and a_{305} (continuous line = model of Eqs. (2)–(4); scattered line = 95% confidence band). All errors are calculated from 95% confidence band. The b value is the intercept of regression that is not used in the model elaboration.

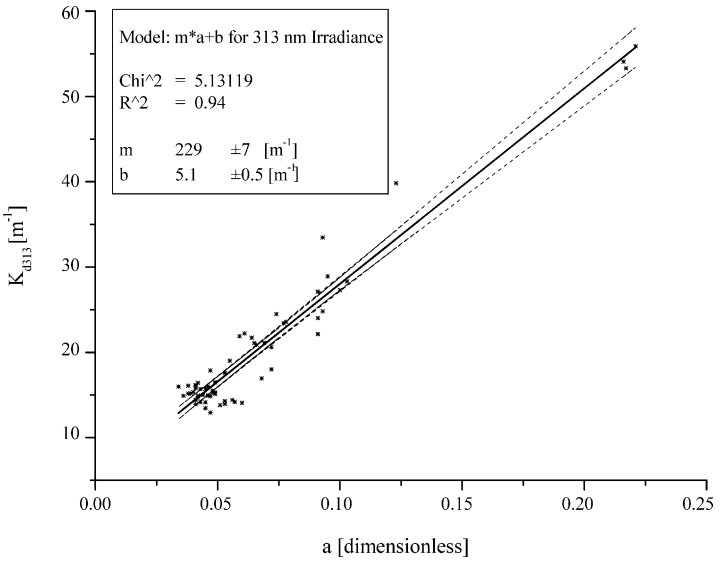

Fig. 6. Linear regression between $K_{d,313}$ and a_{313} (continuous line = model of Eqs. (2)–(4); scattered line = 95% confidence band). All errors are calculated from 95% confidence band. The *b* value is the intercept of regression that is not used in the model elaboration.

lengths followed the theoretical values of $230\,m^{-1}$ (Table 1). The respective difference between the measured and theoretical values ($(m_t - m_\lambda)/m_t = \Delta m_\lambda$) are $\Delta m_{305} = 0.013$, $\Delta m_{313} = 0.004$, $\Delta m_{320} = 0.009$ and $\Delta m_{340} = 0.043$.

Using this attenuation model, it is possible to estimate the contribution of particulate matter to overall attenuation in the water column. The $K_{p,\lambda}$ (m^{-1}) term includes also the attenuation of the water molecules, which is wavelength dependant but will not vary from

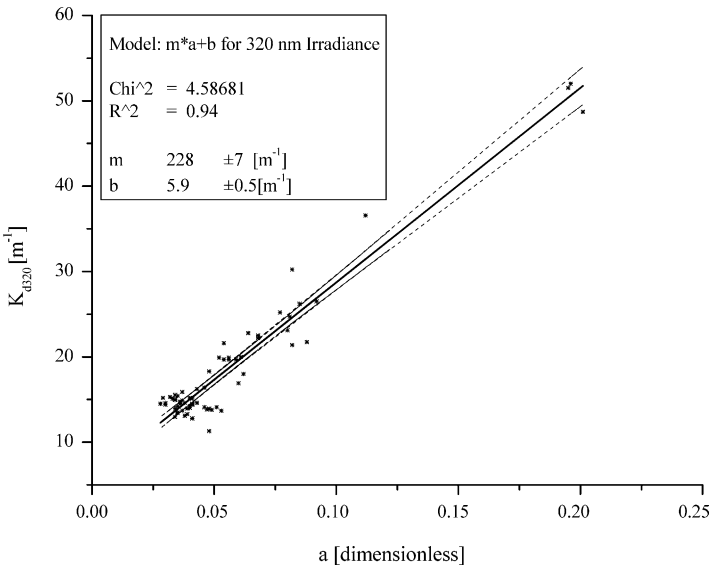

Fig. 7. Linear regression between $K_{d,320}$ and a_{320} (continuous line = model of Eqs. (2)–(4); scattered line = 95% confidence band). All errors are calculated from 95% confidence band. The *b* value is the intercept of regression that is not used in the model elaboration.

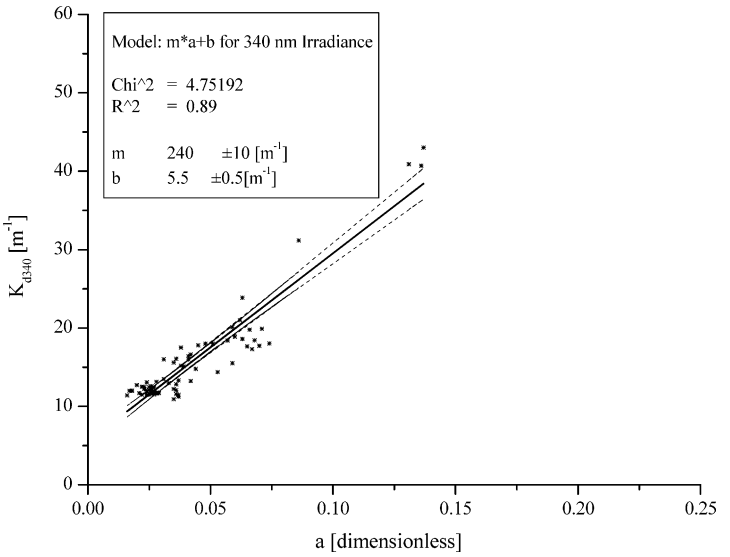

Fig. 8. Linear regression between $K_{d,340}$ and a_{340} (continuous line = model of Eqs. (2)–(4); scattered line = 95% confidence band). All errors are calculated from 95% confidence band. The *b* value is the intercept of regression that is not used in the model elaboration.

Table 1
Angular coefficients for the theoretical dependence between $K_{d,\lambda}$ and a_λ and from linear regression (see Figs. 5–8) for any measured wavelength

m_t (m^{-1})	230
m_{305} (m^{-1})	227 ± 8
m_{313} (m^{-1})	229 ± 7
m_{320} (m^{-1})	228 ± 7
m_{340} (m^{-1})	240 ± 10

The errors are calculated from 95% confidence band (Origin 6.0).

site to site. Kirk (1994) reports that the absorption of the pure water in these UV spectrum ranges is less than 1% of the values of $K_{p,\lambda}$ that are reported here. Therefore, Eq. (4) separates the measured total attenuation coefficient into the dissolved fraction (A_λ) and the particulate fraction ($K_{p,\lambda}$), this latter being the residual from the subtraction of the A_λ from the total vertical attenuation coefficient. This value varies from station to station and from wavelength to wavelength according to the quantity and quality of the particulate matter.

5. Discussion

Organic matter is an important component of most tropical and subtropical lakes. This is partially due to the high incident solar radiation and rainfall, which allow high primary organic production. In such environments, high molecular weight humic substances are formed by the oxidation and polymerisation of lignin (and other phenolic compounds) in decomposing plant tissue. In some water bodies, the source of most humic materials is runoff water that is leached from the surrounding catchments. In the wetland ecosystems, floating border vegetation provides a significant source of decomposing plant matter, increasing the concentrations of dissolved organic matter in the open waters Stevenson (1982). These components are the major responsible of the attenuation in the shorter wavelength of the solar spectrum (in particular in the UVB Hautala et al., 2000). To determine the sensitivity of the total attenuation coefficient to changes in the dissolved material fraction of the water column, the above model may be used. The attenuation coefficients ($K_{d,\lambda}$, A_λ and $K_{p,\lambda}$) depend on wavelength: shorter wavelengths are more sensitive to dissolved matter than higher wavelengths. To evaluate the relation between wavelengths, dissolved and particulate matter on the attenuation coefficient for downward radiation ($K_{d,\lambda}$), Eq. (5) was used.

$$P_\lambda = \frac{K_{p,\lambda}}{K_{d,\lambda}} = \frac{K_{d,\lambda} - A_\lambda}{K_{d,\lambda}} = 1 - \frac{A_\lambda}{K_{d,\lambda}} \quad (5)$$

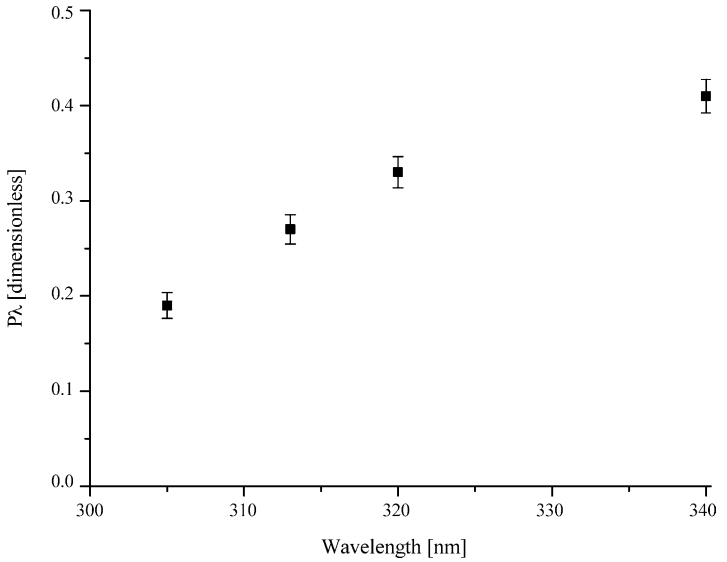

Fig. 9. Contribution of particulate matter to UV attenuation in relation of wavelength. The points are average values of percentage of P_λ calculated from Eq. (5) for all sites. The errors are standard deviations. The effect of the dissolved matter was high in shorter wavelength but it is not possible neglect the effect of the particulate matter that increasing in importance with increasing the wavelength.

Eq. (5) quantify the relative importance of the dissolved and particulate matter in the attenuation of solar UV radiation. For all wavelengths measured, the average and standard deviation of the P_λ values on the 77 stations is reported in Fig. 9.

Spatial variation of the UV attenuation is to be expected in natural aquatic ecosystems, in the proximity of the areas where dissolved and particulate matter are released. Changes of the optical proprieties can be measured and the percentage of each component (dissolved and particulate) in the overall $K_{d,\lambda}$. This is best demonstrated using a geographical representation of the measured and estimated values. The estimated spatial distributions attenuation due to the dissolved fraction (A_λ) and the particulate fraction ($K_{p,\lambda}$) are presented in Figs. 10–13. As each fraction will degrade in time through photo-induced and bacteriological degradation, the areas of the highest attenuation are those areas where the source of dissolved and particulate matter are most likely present.

There is no clear relation between the attenuation of the two fractions as the spatial distributions of A_λ and $K_{p,\lambda}$ showed. The southern part of the lake shows an extremely high attenuation due to the dissolved fraction but a low attenuation due to the particulate fraction. The inflow of a small river in this area of the lake is the most probable cause of these dissolved materials. The river, the Rio Mirinay, drains a small wetland area with bordering agricultural fields. The loss of the particulate fraction of this slow moving river water may occur before reaching the lake waters. The central area of the northern basin showed a less homogeneous pattern, particularly regarding the particulate fraction. This basin is more susceptible to wind induced resuspension due to its morphology (Cozar et al., 2005). The values of A_λ and $K_{p,\lambda}$ in the maps show similar results in the higher wavelengths (320 and 340 nm; Fig. 9).

The use of a model that separates the attenuation due to the dissolved and particulate fractions is an important tool in the analysis of the underwater radiation environment of aquatic ecosystems. As each fraction will have different residence times and different biological fates. Dissolved matter is can be incorporated into the microbial food chain. On the other hand, the plankton components are a relevant part of the particulate matter. In fact, the southern basin (higher A_λ) shows the highest concentrations of the microbial chain components and the northern basin (higher $K_{p,\lambda}$) shows the highest concentrations of phytoplankton (Cozar et al.,

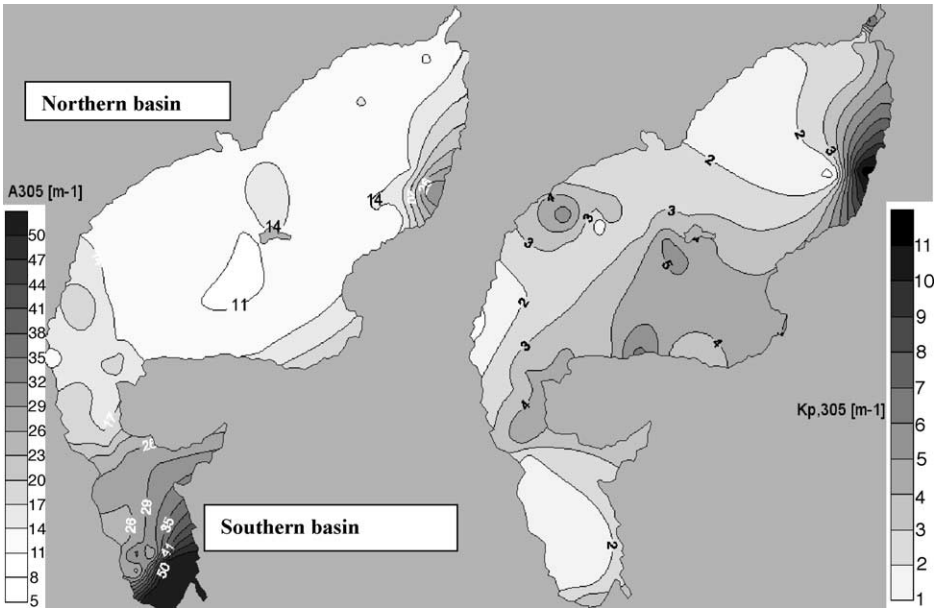

Fig. 10. Maps representation of A_{305} and $K_{p,305}$ in the *Laguna Iberá* using Kriging interpolation method (Surfer 7.0).

2003). The interaction between the UV radiation and the dissolved organic matter can form photo-products that could be potentially harmful for the phytoplankton community in relation to the biomass or the functionality (Zagarese et al., 2001). This process supports the relative low values of the phytoplankton concentration measured in the southern basin.

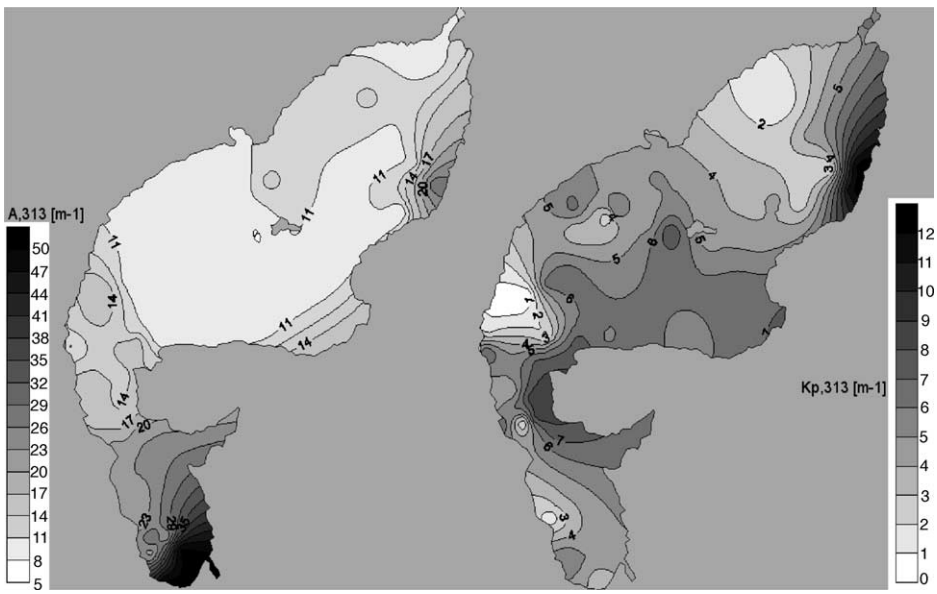

Fig. 11. Maps representation of A_{313} and $K_{p,313}$ in the *Laguna Iberá* using Kriging interpolation method (Surfer 7.0).

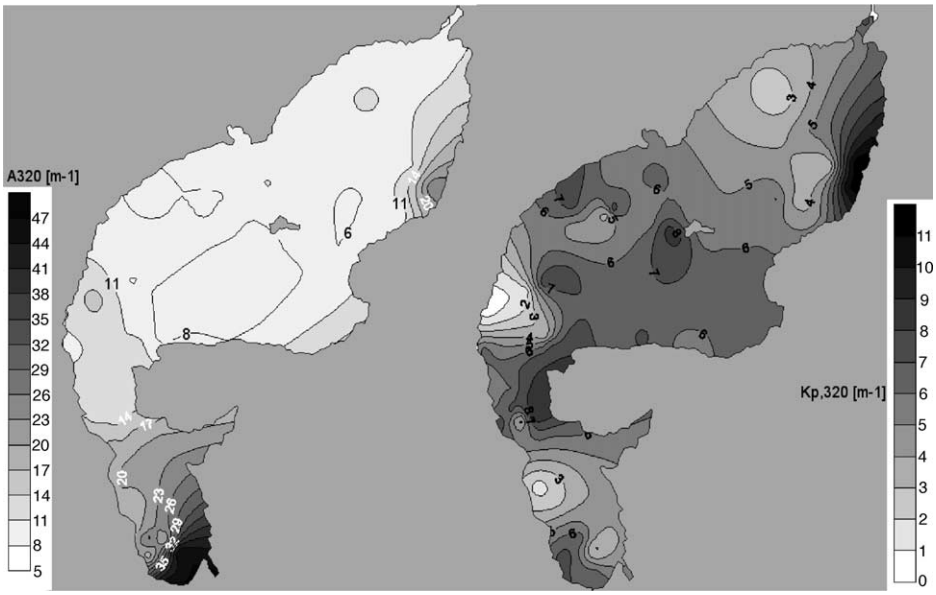

Fig. 12. Maps representation of A_{320} and $K_{p,320}$ in the *Laguna Iberá* using Kriging interpolation method (Surfer 7.0).

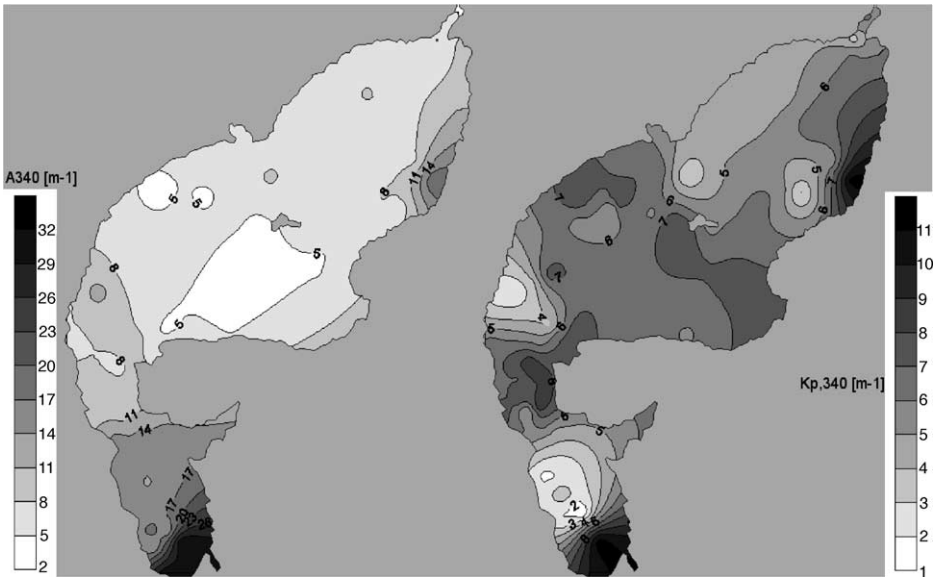

Fig. 13. Maps representation of A_{340} and $K_{p,340}$ in the *Laguna Iberá* using Kriging interpolation method (Surfer 7.0).

6. Conclusion

In the present work, the relation between UV attenuation and dissolved and particulate fractions of the water column was analyzed. The studied wetland lake was found to be characterized by high spatial variation of both dissolved and particulate matter. The attenuation model that was determined, from in situ and laboratory measurements, showed the individual contribution to overall attenuation by each component. The

good fit of the linear regression (Figs. 5–8) allowed for the definition of two optical parameters (A_λ and $K_{p,\lambda}$). These parameters describe the attenuation of the dissolved (e.g. humic acids) and particulate matter (e.g. phytoplankton) in the aquatic ecosystem. The high importance of the dissolved matter to attenuate the shorter wavelengths (305 and 313 nm) is well confirmed. Interestingly, the contribution of the particulate fraction is quite significant, in particular at high wavelength of the solar UV measured spectrum (320 and 340 nm). The spatial representation of the model output (A_λ and $K_{p,\lambda}$) was showed the distribution of dissolved and particulate matter and the spatial difference of UV attenuation in the aquatic environments.

The inclusion of optical measurements (and the described model) into monitoring programmes offers useful information about the dynamics of the aquatic ecosystems characteristics (dissolved and particulate matter) and in relation also the changing global and local UV exposure.

Acknowledgements

This project is supported through the European Commission Directorate General XII INCO programme (ERB I18 CT98 0262). We would like to thank the park guards of *Reserva Provincial del Iberá* for their assistance in data gathering and the Iberá Project team for their fruitful collaboration. The research was supported by the Italian Interuniversity Consortium CSGI.

References

Amyot, M., Mierle, G., Lean, D., McQueen, D., 1997. Effect of solar radiation on the formation of dissolved gaseous mercury in temperate lakes. Geochim. et Cosmochim. Acta 61, 975–987.

Bothwell, M.L., Sherbot, D.M.J., Pollock, C.M., 1994. Ecosystem response to solar ultraviolet-B radiation: influence of trophic-level interactions. Science 265, 97–101.

Bracchini, L., Cozar, A., Dattilo, A.M., Falcucci, M., Gonzales, R., Loiselle, S., Hull, V., 2004a. Analysis of extinction in ultraviolet and visible spectra of water bodies of the Paraguay and Brazil wetlands. Chemosphere 57, 1245–1255.

Bracchini, L., Loiselle, S.A., Dattilo, A.M., Mazzuoli, S., Cózar, A., Rossi, C., 2004b. The spatial distribution of the optical properties in the UV and visible in an aquatic ecosystem. Photochem. Photobiol. 80 (1), 139–149.

Cozar, A., Galvez, J.A., Hull, V., Garcia, C.M., Loiselle, S.A., 2005. Sediment resuspension by wind in a shallow lake of Esteros del Ibera (Argentina): a model based on turbidimetry. Ecol. Mod. 186, 63–76.

Cozar, A., Garcia, C.M., Galvez, J.A., 2003. Analysis of plankton size spectra irregularities in two subtropical shallow lakes (Esteros del Ibera, Argentina). Can. J. Fish. Aquat. Sci. 60, 411–420.

Dattilo, A.M., Bracchini, L., Carlini, L., Loiselle, S.A., Rossi, C., 2005a. The estimate of the effects of UV radiation on mortality of *Artemia franciscana* in naupliar and adult stages. Int. J. Biometeorol.

Dattilo, A.M., Decembrini, F., Bracchini, L., Focardi, S., Mazzuoli, S., Rossi, C., 2005b. Penetration of solar radiation into waters of Messina Strait (Italy). Ann. Chim.-Rome., 95.

Hader, D.P., Kumar, H.D., Smith, R.C., Worrest, R.C., 1998. Effects on aquatic ecosystems. J. Photochem. Photobiol. 46, 53–68.

Hakkinen, J., Pasanen, S., V., Kukkonen, J., 2001. The effects of solar UV-B radiation on embryonic mortality and development in three borealis anurans (*Rana temporaria*, *Rana arvalis* and *Bufo bufo*). Chemosphere 44, 441–446.

Hautala, K., Peuravuori, J., Pihlaja, K., 2000. Measurement of aquatic humus content by spectroscopic analyses. Water Res. 34, 246–258.

Kirk, J.T.O., 1977. Use of a quanta meter to measure attenuation and underwater reflectance of photosynthetically active radiation in some inland and costal South-eastern Australian waters. Aust. J. Freshwater Res. 28, 9–21.

Kirk, J.T.O., 1994. Optics of UV-B radiation in natural waters. In: Williamson, C.E., Zagarese, H.E. (Eds.), Impact of UV-B Radiation on Pelagic Freshwater Ecosystems. Schweizerbart, Stuttgart, pp. 1–16.

Kirk, J.T.O., Hargreaves, B.R., Morris, D.P., Coffin, R.B., David, B., Frederickson, D., Karentz, D., Lean, D.R.S., Lesser, M.P., Mandronich, S., Morrow, J.H., Nelson, N.B., Scully, N.M., 1994. Measurements of UV-B radiation in two freshwater lakes: an instrument intercomparison. In: Williamson, C.E., Zagarese, H.E. (Eds.), Impact of UV-B Radiation on Pelagic Freshwater Ecosystems. Schweizerbart, Stuttgart, pp. 71–99.

Morris, D.P., Zagarese, H., Williamson, C.E., Balseiro, E.G., Hargreaves, B.R., Modenutti, B., Moller, R., Quimalinos, C., 1995. The attenuation of solar UV radiation in lakes and the role of dissolved organic carbon. Limnol. Oceanogr. 40 (8), 1381–1391.

Nieke, B., Reuter, R., Heuermann, R., Wang, H., Babin, M., Therriault, J.C., 1997. Light absorption and fluorescence properties of chromophoric dissolved organic matter (CDOM), in the St. Lawrence Estuary (Case 2 Water). Continental Shelf Res. 17, 235–252.

Pienitz, R., Vincent, W.F., 2000. Effect of climate change relative to ozone depletion on UV exposure in subartic lakes. Nature 404, 484–487.

Schindler, D.W., Curtis, P.J., Parker, B.R., Stainton, M.P., 1996. Consequences of climate warming and lake acidification for UV-B penetration in North American boreal lakes. Nature 379, 705–708.

Smith, R.C., Baker, K.S., 1978. Penetration of UV-B and biologically effective dose rate in natural waters. Photochem. Photobiol. B: Biol. 29, 311–323.

Stevenson, F.J., 1982. Humus Chemistry: Genesis, Composition, Reactions. Wiley, New York, pp. 195–219.

Yan, N.D., Keller, W., Scully, N.M., Lean, D.R.S., Dillon, P.J., 1996. Increased UV-B penetration in lake owing to drought-induced acidification. Nature 381, 141–143.

Zagarese, H.E., Diaz, M., Pedroso, F., Ferraro, M., Cravero, W., Tartarotti, B., 2001. Photodegradation of natural organic matter exposed to fluctuting levels of solar radiation. J. Photochem. Photobiol. B: Biol. 61, 35–45.